Structure of Particle-Laden Jets: Measurements and Predictions

J-S. Shuen,* A. S. P. Solomon,* Q-F. Zhang,† and G. M. Faeth‡
The Pennsylvania State University, University Park, Pennsylvania

Mean and fluctuating velocities of both phases as well as particle mass fluxes were measured in turbulent, dilute, monodisperse, particle-laden jets injected into a still environment. The new measurements were used to evaluate a stochastic separated flow model of the process that treated effects of interphase slip and turbulent dispersion using random-walk computations for particle motion. The continuous phase was treated using a modified k-ϵ model allowing for direct contributions of interphase transport of both mean and turbulence properties. The model performed reasonably well over the new data base, with all empirical parameters fixed from earlier work. In constrast, simplified models ignoring either interphase slip or turbulent dispersion yielded poor agreement with the measurements.

Nomenclature

a = acceleration of gravity
C_D = drag coefficient
C_i = parameters in turbulence model
d = injector diameter
d_p = particle diameter
G = particle mass flux
k = turbulence kinetic energy
L_e = dissipation length scale
m_p = particle mass
n = number of particle groups
$\dot{n}_i$ = number of particles per unit time in group i
r = radial distance
Re = Reynolds number
S_ϕ = source term
$S_{p\phi}$ = source term due to particles
t = time
t_e = eddy lifetime
u = axial velocity
$\boldsymbol{u}$ = velocity vector
$\boldsymbol{u}_p$ = particle velocity vector
v = radial velocity
V_j = volume of computational cell j
x = axial distance
$\boldsymbol{x}_p$ = particle position vector
Δx_p = relative path length of particles in an eddy
Δt_p = time of particle residence in an eddy
ϵ = rate of dissipation of turbulence kinetic energy
μ_t = turbulent viscosity
ρ = density
σ_i = turbulent Prandtl/Schmidt number
ϕ = generic property

Subscripts

c = centerline quantity
p = particle property
0 = injector exit condition
∞ = ambient condition

Superscripts

$(\ \_\ )'$ = fluctuating quantity
$(\ \bar{}\ )$ = time mean value

Introduction

THE objective of this investigation was to complete measurements useful for evaluation of models of the structure of particle-laden jets. The experiments involved turbulent, dilute, monodisperse, particle-laden jets injected into a still environment. This arrangement facilitates model evaluation since it has a simple geometry, well-defined boundary conditions, and satisfies the boundary-layer approximations. The results are also of interest for developing models of sprays, since the present flows exhibit many processes encountered in sprays while avoiding complications due to polydisperse drop sizes and drop coalescence. The new data was also used to begin evaluation of models typical of recent spray analysis.

Earlier theoretical and experimental investigations of particle-laden jets have recently been reviewed[1] and this discussion will not be repeated here. The present investigation is primarily an extension of earlier work at The Pennsylvania State University where models of particle-laden jets were developed and evaluated using existing measurements.[2,3] Three models were considered: 1) a locally homogeneous flow (LHF) model, where velocities and turbulent mixing properties of both phases were taken to be the same; 2) a deterministic separated flow (DSF) model, where interphase slip was considered but effects of turbulence on particle motion were ignored; and 3) a stochastic separated flow (SSF) model where effects of both interphase slip and turbulence on particle motion were considered using random-sampling techniques. In general, the LHF and DSF models over- and underestimated rates of particle spread and flow development, respectively. In constrast, the SSF model yielded encouraging predictions of flow structure. An exception was at high particle mass loadings, where effects of particles on turbulence properties, termed turbulence modulation by Al Taweel and Landau[4] and not considered in the theory, were felt to be responsible for the deficiency.[3] Unfortunately, this evaluation was limited by insufficient information concerning initial conditions and incomplete structure measurements for the existing data base. The present investigation seeks to partially rectify these limitations by providing more complete data for model evaluation. Effects of turbulence modulation are also considered in order to estimate its influence on present results.

Elghobashi and co-workers[5-7] perceived the same difficulties and recently reported new theoretical and ex-

Received Nov. 21, 1983; revision received April 11, 1984.

*Research Assistant, Department of Mechanical Engineering.
†Adjunct Lecturer, on leave from Department of Aero-Engine, Nanjing Aeronautical Institute, Nanjing, China.
‡Professor, Department of Mechanical Engineering. Member AIAA.

perimental results for particle-laden jets. The present investigation complements this work. The analysis of Elghobashi and Abou-Arab[5] employs time averaging, assuming particle drag in the Stokes flow regime, to treat interactions between the phases. In contrast, the present analysis allows for nonlinear interphase processes, which are frequently encountered in practice, using stochastic methods. Furthermore, the experiments of Elghobashi and coworkers[6,7] treat particle-laden jets discharging into a slow coflow of air within a round duct. In contrast, the present measurements are in a still environment which simplifies specification of boundary conditions. Evaluation of the present model using the data of Refs. 6 and 7 will be the subject of a separate publication.

In the following, the experimental methods are presented first. This is followed by a description of the comparison between predictions and measurements. All aspects of the study are described only briefly. Full details and a tabulation of all data are provided by Shuen et al.[8]

Experimental Methods

Test Apparatus

The particle-laden jet was directed vertically downward within a screened enclosure (16-mesh screen, 1 m square by 2.5 m high). The injector could be traversed vertically and in one lateral direction. Traversing the third dimension, to obtain radial profiles of flow quantities, involved moving the entire cage assembly which was mounted on a track. This arrangement allowed rigid mounting of optical instrumentation.

The jet tube had an inside diameter of 10.9 mm and extended vertically downward for 90 injector diameters. This yielded symmetric property profiles at the jet exit. The initial conditions of both phases were measured at the jet exit.[8]

Airflow through the injector from an oil-free compressor was metered with critical-flow orifices. Sand particles for the particle-laden jet experiments were introduced by a gear feeder powered with a variable-speed motor. Properties of the particles and details of the five test conditions are summarized in Table 1. Particle size distributions were measured using a microscope with a sample of more than 1000 particles for each size group.[8]

Instrumentation

Gas Velocity

Mean and fluctuating gas velocities were measured with a single-channel, frequency-shifted He-Ne laser Doppler anemometer (LDA) having an ellipsoidal measuring volume (98 μm in diameter, 470 μm long) with a fringe spacing of 3.13 μm. Both the jet and the surroundings were seeded (0.2 μm aluminum oxide particles) to eliminate concentration bias.[8] Various velocity components and turbulence quantities were measured by rotating the beam plane. Bias from particles was minimized by rejecting large-amplitude Doppler signals and using seeding particle concentrations more than two orders of magnitude larger than test particle concentrations. Time averages of mean and fluctuating quantities were measured using a burst counter processor (time-averaging mode with high signal rate) in conjunction with a true rms meter and integrating digital voltmeter.

Particle Velocity

Mean and fluctuating particle velocities were measured using the same LDA, but with no seeding particles and low detector gain so that only strong scattering signals from test particles were observed. The burst counter output was collected and processed using a MINC 11/23 minicomputer to yield mean and fluctuating particle velocities (taken as particle averages).

The centerline particle velocities were checked using a double-flash imaging technique (see Ref. 9). Mean velocities agreed within 5% (case 1) and 15% (cases 2 and 3), but the LDA measurements were significantly lower (40-60%) than the double-flash measurements for the case 4 jet. This behavior was felt to be due to the very large pedestal signal from the large particles of the case 4 jet which reduced signal-to-noise ratio. Therefore, the double-flash results, which are felt to be more reliable, are used for the case 4 jet, while the LDA measurements are used for the other jets.

Particle Drag

The larger sized particles were somewhat irregular. Therefore, particle drag properties were found for a typical sample by measuring free-fall terminal velocities with the LDA. The ratio of the particle drag, assuming a diameter equal to the Sauter mean diameter (SMD) of the sample, and the standard drag coefficient for spheres was found and is summarized in Table 1. This ratio was applied to the particle drag coefficient during the calculations. This procedure is consistent, since computations were conducted assuming monodisperse particles having a diameter equal to the SMD.

Particle Mass Flux

Particle fluxes were measured by isokinetic sampling at the mean gas velocity with a probe inlet of 3 mm diam.[8,10] Samples collected on a filter were weighed after collection for a timed period.

Uncertainties

Uncertainties in mean and fluctuating gas velocities are estimated to be less than 10% and were repeatable within 5%. Mean and fluctuating particle velocities found by the LDA were checked by calibration at several conditions, indicating uncertainties less than 15% for results reported here. Mass conservation checks for particle flow rates were satisfied

Table 1 Summary of test conditions[a]

Parameter	Single phase air jet	Particle-laden jets			
		Case 1	Case 2	Case 3	Case 4
Particle properties:					
Sauter mean diameter, μm	—	79	119	119	207
Diameter standard deviation, μm	—	18	19	19	24
Drag ratio[b]	—	1.00	1.25	1.25	1.51
Loading ratio[c]	0	0.20	0.20	0.66	0.66
Jet exit velocity,[d] m/s	0	24.1	24.2	21.9	18.5
Jet exit mass flux, kg/m^{2}s	0	6.06	6.50	18.9	19.0
Air velocity,[d] m/s	32.1	26.1	29.9	25.2	25.3

[a] Ambient temperature and pressure, 296 K, 97 kPa; injector inside diameter, 10.9 mm; particle density, 2620 kg/m^3.
[b] Particle drag/drag of smooth sphere having the same diameter.
[c] Ratio of injected particle mass flow rate to air flow rate.
[d] Centerline velocity measured at $x/d = 1$.

within 13%, suggesting a similar uncertainty for particle mass flux measurements.

Theoretical Methods

General Description

The boundary-layer assumptions for a steady, axisymmetric, dilute, particle-laden, turbulent jet in an infinite stagnant environment were used in the analysis. A k-ϵ turbulence model was employed to find mean and turbulent properties of the continuous phase, since this approach yielded good predictions for both constant- and variable-density jets during earlier work.[2,3,11-13] For present test conditions, injector exit Mach numbers were less than 0.3; therefore, kinetic energy, viscous dissipation, and gas density variations were neglected with little error. Molecular transport was also ignored, since Reynolds numbers (defined similar to Ref. 2) for present test conditions exceed 10^4.

The LHF and DSF models will be described only briefly since present calculations generally follow past practice.[1-3] However, the SSF model was significantly modified to treat effects of turbulence modulation; therefore, the new formulation will be presented.

Continuous Phase (SSF Formulation)

The present turbulent flow model is based on an approach used by Lockwood and Naguib[13] for single-phase jets and subsequently employed during earlier work at Pennsylvania State University.[11,12] Mean quantities are found by solution of the governing equations for conservation of mass and momentum in conjunction with second-order turbulence model equations for turbulence kinetic energy and its rate of dissipation. The volume fraction of the particle phase is neglected, since void fractions for the test flows exceed 99.9%. The gas density was also constant:

$$\frac{\partial}{\partial x}(\rho\bar{u}\phi)+\frac{1}{r}\frac{\partial}{\partial r}(r\rho\bar{v}\phi)=\frac{1}{r}\frac{\partial}{\partial r}\left(r\frac{\mu_t}{\sigma}\frac{\partial\phi}{\partial r}\right)+S_\phi+S_{p\phi} \qquad (1)$$

The parameters ϕ, S_ϕ, and $S_{p\phi}$ appearing in Eq. (1) are summarized in Table 2, along with appropriate empirical constant. $S_{p\phi}$ and $C_{\epsilon 3}$ result from particle interactions and will be discussed later. The remaining terms and empirical constants were established in single-phase flows.[11-13] The turbulent viscosity was calculated as usual:

$$\mu_t = C_\mu \rho k^2/\epsilon \qquad (2)$$

The flow leaving the injector was similar to fully developed flow and had no potential core. The boundary conditions for Eq. (1) then become:

$$r=0,\quad \frac{\partial\phi}{\partial r}=0; \qquad r\to\infty,\quad \phi=0 \qquad (3)$$

Table 2 Source terms in governing equations

ϕ	S_ϕ	$S_{p\phi}$
1	0	0
$\bar{u}$	0	$\bar{S}_{pu}$
k	$\mu_t\left(\frac{\partial\bar{u}}{\partial r}\right)^2-\bar{\rho}\epsilon$	$\overline{uS}_{pu}-\bar{u}\bar{S}_{pu}$
ϵ	$C_{\epsilon 1}\mu_t\frac{\epsilon}{k}\left(\frac{\partial\bar{u}}{\partial r}\right)^2-C_{\epsilon 2}\bar{\rho}\frac{\epsilon^2}{k}$	$-2C_{\epsilon 3}\mu_t\frac{\epsilon}{k}\frac{\partial\bar{S}_{pu}}{\partial r}$

C_μ	$C_{\epsilon 1}$	$C_{\epsilon 2}$	$C_{\epsilon 3}$	σ_k	σ_ϵ
0.09	1.44	1.87	0.1-5.0	1.0	1.3

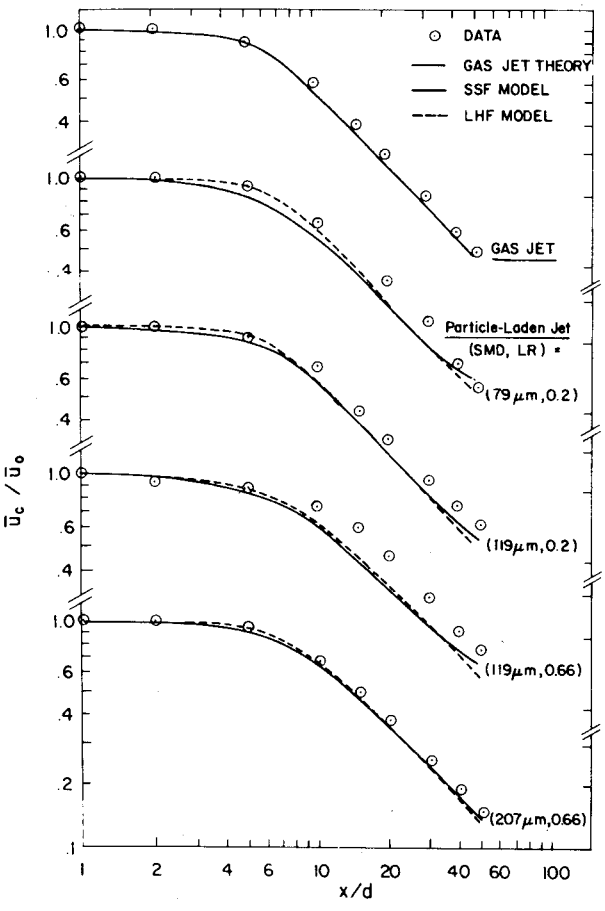

Fig. 1 Axial variation of centerline mean gas-phase velocity.

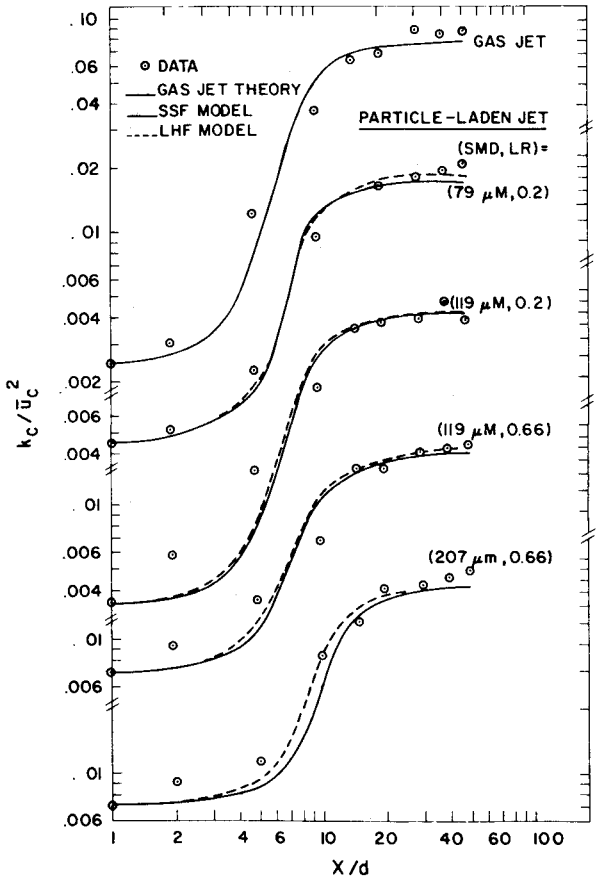

Fig. 2 Axial variation of centerline gas-phase turbulent kinetic energy.

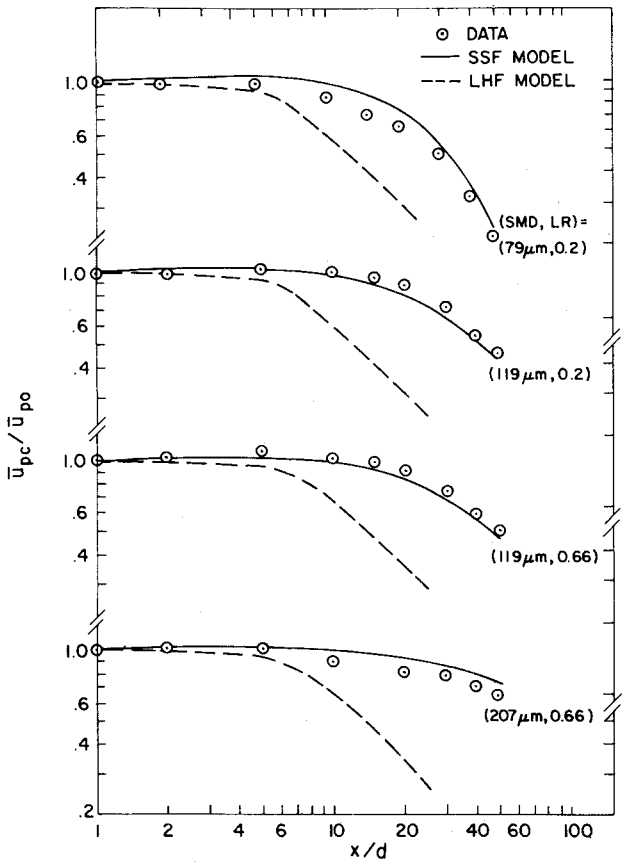

Fig. 3 Axial variation of centerline mean solid-phase velocity.

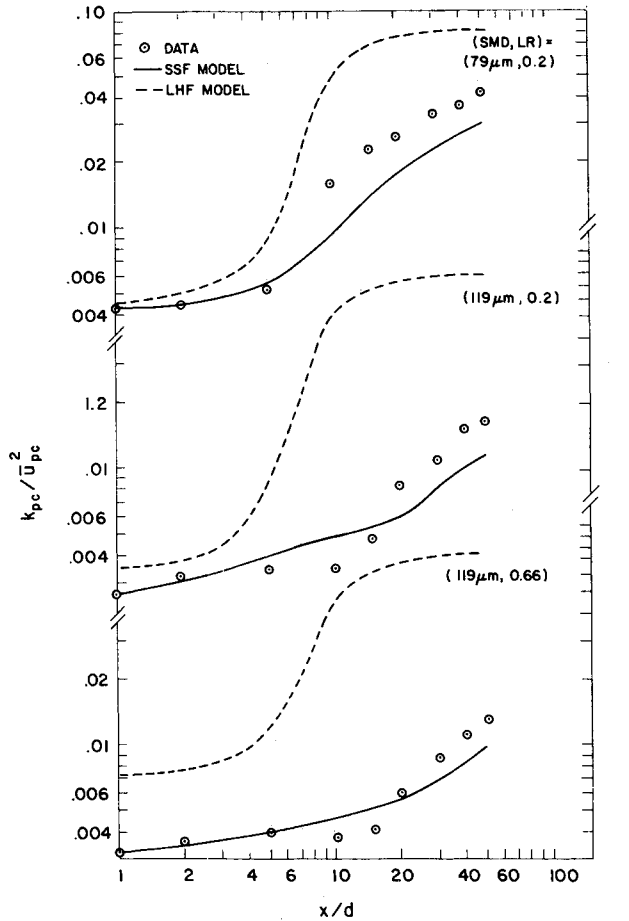

Fig. 4 Axial variation of centerline solid-phase turbulent kinetic energy.

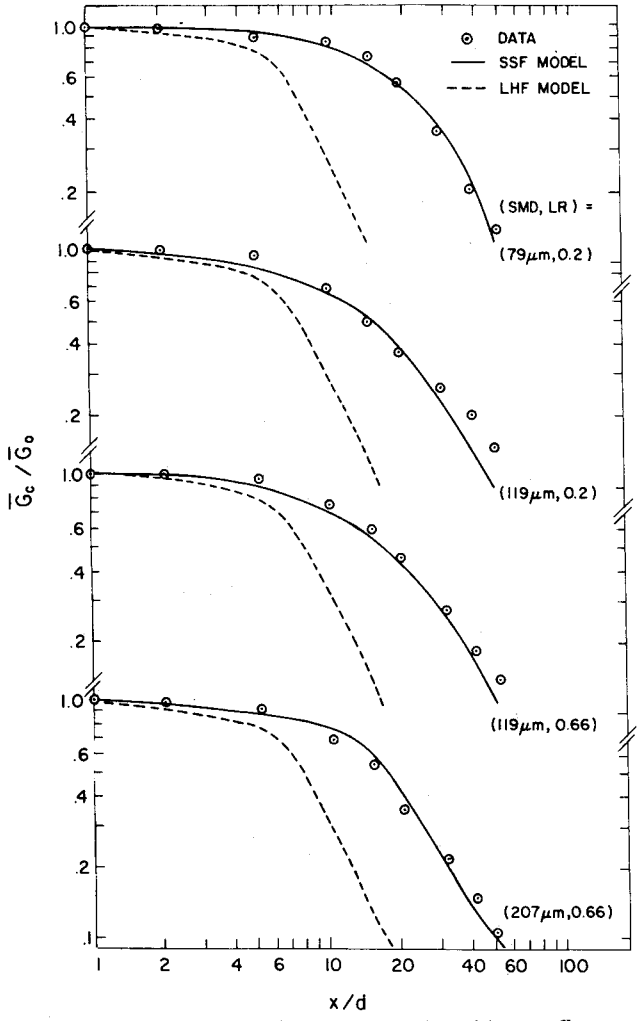

Fig. 5 Axial variation of centerline mean particle mass flux.

Initial conditions were measured at $x/d=1$ and are tabulated in Ref. 8. At $x/d=1$, $\tilde{u}_0$ was measured and $\tilde{v}_0=0$; u' and v' were measured and w' was assumed to be equal to v' to compute k_0; given k_0, ϵ_0 was calculated from measurements of the Reynolds stress and the mean velocity gradient using Eq. (2).

Dispersed Phase (SSF Formulation)

The dispersed phase was treated by solving Lagrangian equations for the trajectories of a statistically significant sample of individual particles (n groups defined by initial position, velocity, and sample) as they move away from the injector and encounter a random distribution of turbulent eddies. This approach provides a means of treating effects of turbulent fluctuations on particle drag and dispersion, as well as effects of particles on turbulence properties.

Key elements of the SSF model are the methods used to specify eddy properties and the time of interaction of a particle with a particular eddy. The present approach involves modification and extension of methods reported by Gosman and Ioannides.[14] Properties are assumed to be uniform within each eddy and to randomly change from one eddy to the next. At the start of particle-eddy interaction, the velocity of an eddy is found by making a random selection from the probability density function (pdf) of velocity [taken to be an isotropic Gaussian pdf having standard deviations $(2k/3)^{1/2}$ and mean values $\tilde{u}$, $\tilde{v}$, and $\tilde{w}=0$].[1-3] A particle is assumed to interact with an eddy for a time which is the minimum of either the eddy lifetime or the time required for a particle to cross an eddy. These times are estimated, assuming that the

characteristic size of an eddy is the dissipation length scale

$$L_e = c_\mu^{3/4} k^{3/2}/\epsilon \tag{4}$$

and that the eddy lifetime is

$$t_e = L_e/(2k/3)^{1/2} \tag{5}$$

Therefore, particles are assumed to interact with an eddy as long as both the time and the relative distance of interaction satisfy the following criteria[2]:

$$\Delta t_p \leqq t_e, \qquad |\Delta x_p| \leqq L_e \tag{6}$$

Assumptions for particle trajectory calculations are typical of analysis of dilute particle-laden flows[1,9]: drag is treated empirically, assuming quasisteady flow for spherical particles with no influence of nearby particles; particle collisions are neglected; since $\rho_p/\rho > 200$ for present tests, effects of virtual mass, Bassett and Magnus forces are neglected with little error; and static pressure gradients are negligible. Local ambient properties are fixed by instantaneous eddy properties, which implicitly provides for effects of turbulent fluctuations on particle dispersion and drag.

With these asumptions, the position and velocity of each particle group can be found by integrating

$$\frac{dx_{pi}}{dt} = u_{pi} \tag{7}$$

$$\frac{du_{pi}}{dt} = \left(\frac{3\rho C_D}{4 d_p \rho_p}\right)(u_i - u_{pi})\,|u - u_p| + a_i \tag{8}$$

where $i = 1,2,3$ and the velocities shown in these equations are instantaneous velocities for a particular eddy and particle group. Particle Reynolds numbers did not reach the supercritical regime; therefore, the standard drag coefficient for solid spheres was taken as follows[1-3]:

$$C_D = \frac{24}{Re}\left(1 + \frac{Re^{2/3}}{6}\right), \qquad Re \leqq 1000$$

$$= 0.44, \qquad Re > 1000 \tag{9}$$

with C_D multiplied by the drag ratio given in Table 1.

Particle Source Terms

The interaction between particles and the continuous phase yields source terms in the governing equation for conservation of momentum and in the model equations for k and ϵ when turbulence modulation is considered. The source term in the $\bar{u}$ equation is found by computing the net change in momentum as each particle group i passes through the computational cell j

$$S_{pu_j} = V_j^{-1} \sum_{i=1}^{n} \dot{n}_i m_p (u_{pi_{\text{in}}} - u_{pi_{\text{out}}}) \tag{10}$$

where $\dot{n}_i$ is the number of particles per unit time in each group.

Source terms in the governing equations for turbulence quantities were derived following conventional procedures.[15,16] These terms, S_{pk} and $S_{p\epsilon}$, appear in Table 2, while their derivation appears in Ref. 8. Instantaneous properties are known from the SSF formulation; therefore, S_{pk} is exact. The term $S_{p\epsilon}$ is modeled consistent with conventional k-ϵ models, but this introduces one new model constant that must be determined empirically.

Numerical Solution

The calculations for the continuous phase were performed using a modified versionof GENMIX.[17] The computational grid was similar to past work[1-3]: 33 cross-stream grid nodes; streamwise step sizes limited to 6% of the current flow width or an entrainment increase of 5% (whichever was smaller). The dispersed phase was computed using a second-order, finite difference algorithm employing no less than 2000 particle groups.

Simplified Models

DSF Model

Effects of turbulent fluctuations on particle drag and dispersion, as well as effects of turbulence modulation, are ignored for the DSF model. Particle trajectories are found by integrating Eqs. (7) and (8), but the local mean velocity of the continuous phase replaces the instantaneous eddy velocity. Each initial condition yields a single deterministic trajectory; therefore, 200 particle groups sufficed to close the solution numerically. Since turbulent modulation is ignored, $S_{pk} = S_{p\epsilon} = 0$. Effects of particle drag in the mean momentum equation are found from Eq. (10), similar to the SSF calculations.

LHF Model

This approximation implies that both phases have the same instantaneous velocity at each point in the flow; therefore, the flow corresponds to a variable-density single-phase fluid

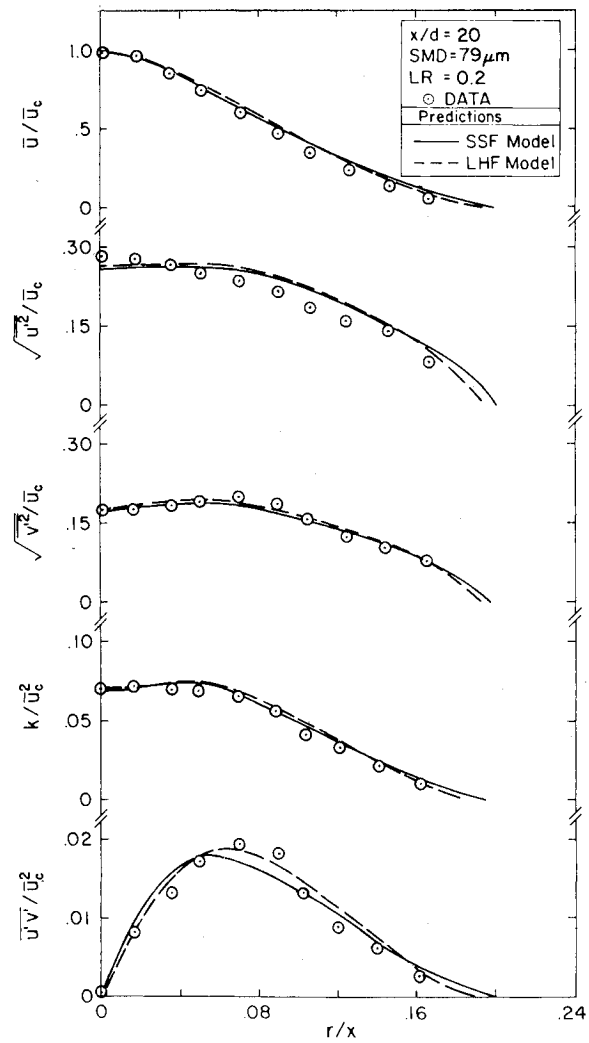

Fig. 6 Radial variation of gas-phase mean and turbulent quantities in case 1 particle-laden jet at $x/d = 20$.

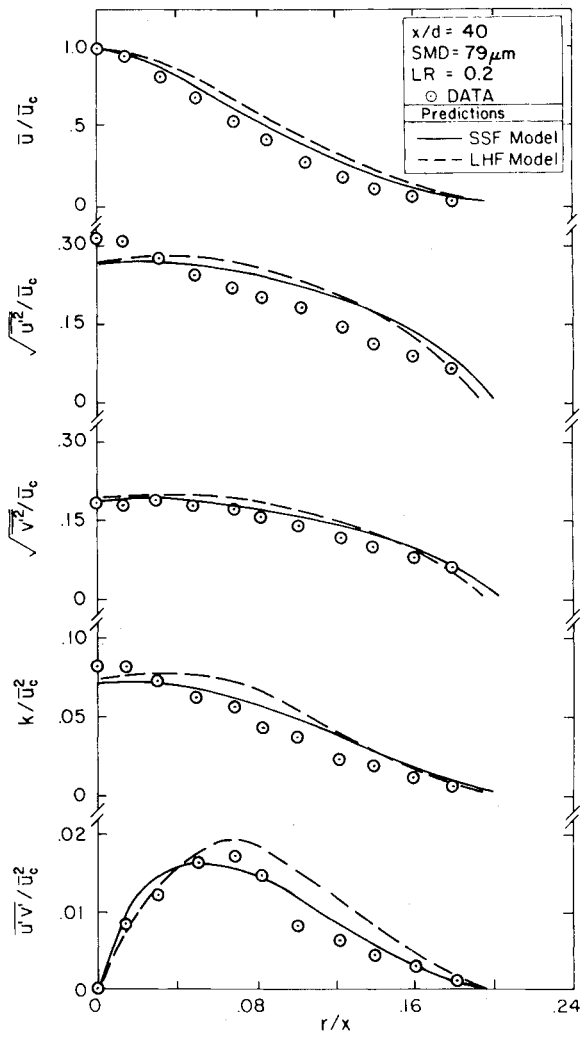

Fig. 7 Radial variation of gas-phase mean and turbulent quantities in case 1 particle-laden jet at $x/d = 40$.

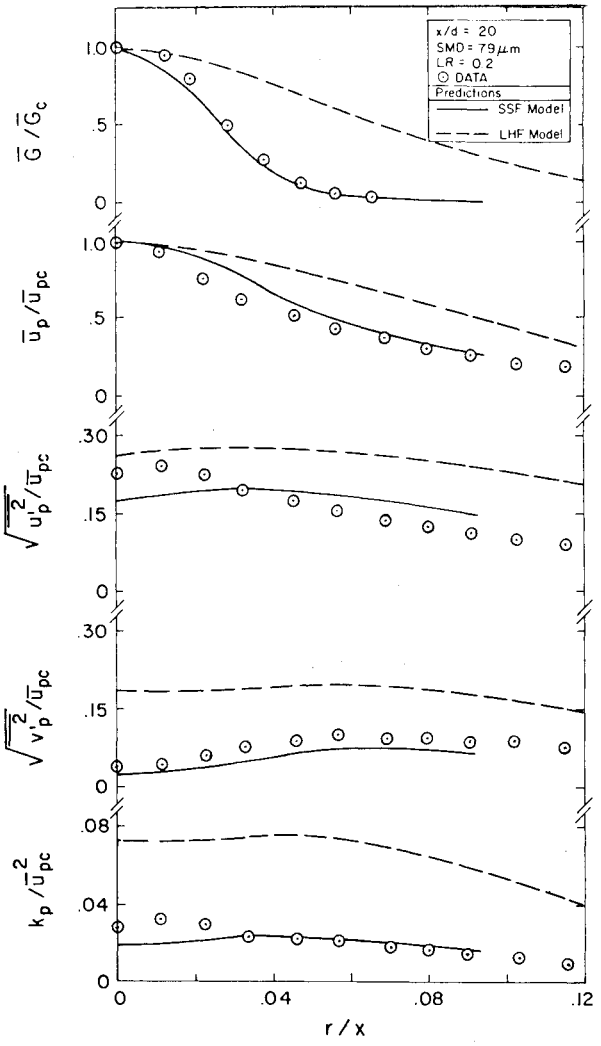

Fig. 8 Radial variation of solid-phase mean and turbulent quantities in case 1 particle-laden jet at $x/d = 20$.

whose density changes due to changes in particle concentration. Turbulent dispersion of particles is then equivalent to that of a gas and particle inertia fully influences turbulence properties; i.e., the method implicitly accounts for effects of turbulence modulation to the extent that the no-slip assumption is correct.

The treatment of the variable-density fluid follows past practice.[1-3] Through the assumption of no-slip, there is no need to compute particle trajectories and all particle source terms in the governing equations for the continuous phase are zero.

Results and Discussion

Axial Variation of Flow Properties

Effects of turbulence modulation were found to be small for present test conditions; therefore, S_{pk} and $S_{p\epsilon}$ were omitted during SSF model predictions shown on the following plots to minimize the intrusion of empiricism. Turbulence modulation is discussed separately at the end of this section.

Gas Phase

Predicted and measured mean gas velocities along the jet axis are illustrated in Fig. 1 for all of the test conditions presented in Table 1. Agreement between predictions and measurements is quite good for the pure gas jet. This establishes a baseline for the particle-laden jets similar to past findings.[1-3,11-13] The predictions of the LHF and SSF models are nearly identical for the particle-laden jets and are in reasonably good agreement with the measurements. Gas velocities decay more slowly for the particle-laden jets at high loading ratios, due to exchange of momentum from the solid phase.

LHF and SSF predictions and measurements of gas-phase turbulence kinetic energy along the axis are illustrated in Fig. 2. There is good agreement between predictions and measurements. The fact that SSF (ignoring turbulence modulation) and LHF predictions (which implicitly consider turbulence modulation) are roughly the same, indicates that effects of turbulence modulation were small in these flows. This is reasonable, since the test flows were dilute.

Particle Phase

Predicted and measured mean particle velocities along the axis are illustrated in Fig. 3. The SSF model predictions are reasonably good. In contrast, the LHF model overestimates the rate of decay of particle velocities, since the particles have significant inertia for these test conditions.

The axial variation of particle turbulence kinetic energy is illustrated in Fig. 4. Results are not shown for the case 4 particle-laden jet due to the problems with the LDA measurements for the large particles which were discussed earlier. The LHF model significantly overestimates particle turbulence levels at all conditions, since the particles cannot actually follow the gas-phase turbulent motion due to their inertia. In contrast, the SSF model is in fair agreement with the measurements.

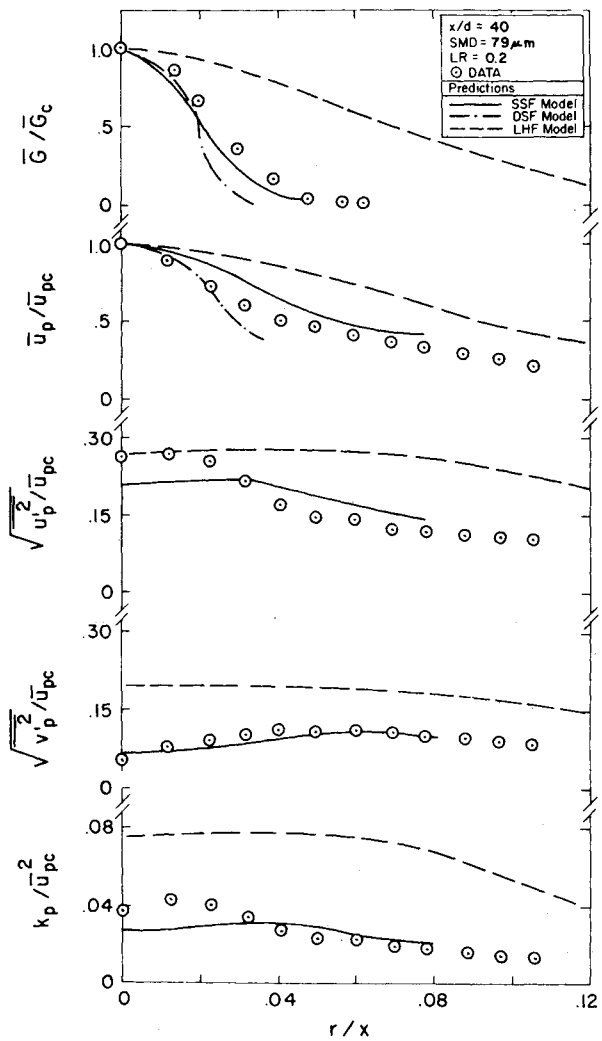

Fig. 9 Radial variation of solid-phase mean and turbulent quantities in case 1 particle-laden jet at $x/d = 40$.

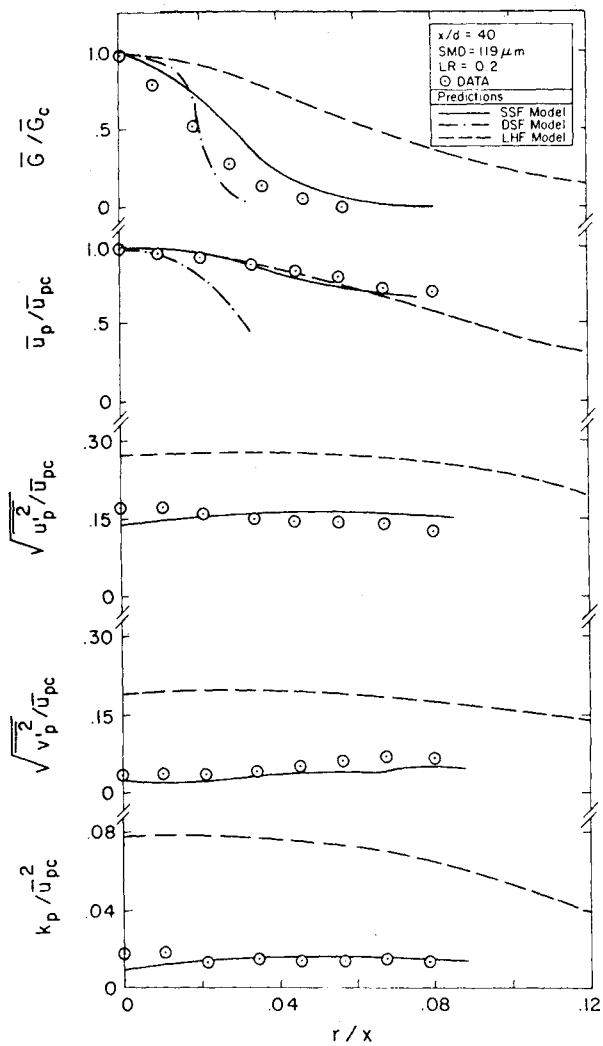

Fig. 10 Radial variation of solid-phase mean and turbulent quantities in case 2 particle-laden jet at $x/d = 40$.

Predicted and measured particle mass fluxes along the axis are illustrated in Fig. 5. The LHF model significantly overestimates particle dispersion, since slip between the phases is neglected, causing overestimation of the rate of decay of particle mass flux with distance from the injector. In contrast, the SSF model yields satisfactory predictions.

Radial Variation of Flow Properties

Gas Phase

Predicted and measured radial profiles of mean and turbulent quantities were in good agreement for the pure gas jet. This behavior was similar to past experience by Shearer et al.[11] and Mao et al.,[12] therefore, those results will not be considered here.

Predicted and measured radial profiles of mean and turbulent gas-phase properties for the case 1 particle-laden jet are illustrated in Figs. 6 and 7 for $x/d = 20$ and 40, respectively. Predictions of the gas-phase fluctuating velocity components were obtained assuming $\tilde{u}'^2 : \tilde{v}'^2 = k : k/2$, which was observed for the present tests and is normally observed for single-phase jets. The case 1 jet has a relatively low loading ratio; therefore, gas-phase properties approach the properties of a single-phase jet. Similar to Figs. 1 and 2, gas-phase properties are relatively independent of model type and both the LHF and SSF models are in reasonably good agreement with the measurements. The LHF model yields higher Reynolds stress levels than the SSF model despite effects of turbulence modulation. This behavior results since the LHF model also overestimates the rate of exchange of momentum between the phases.

Table 3 Summary of sensitivity study[a]

Input parameter	Output variables				
	$\tilde{u}_c$	$k_c/\tilde{u}_c^2$	$\tilde{u}_{pc}$	$k_{pc}/\tilde{u}_{pc}^2$	$\tilde{G}_c$
	Case 1 Particle-laden jet				
ϵ_0	5	0	9	11	8
k_0	−6	2	−8	13	−8
C_D	3	4	−30	28	−16
d_p	6	−4	51	−50	18
	Case 3 Particle-laden jet				
ϵ_0	3	0	6	−6	7
k_0	−6	1	−5	6	−7
C_D	5	3	−31	19	−14
d_p	5	−2	30	26	16

[a]Entries show percent change in prediction at $x/d = 40$ by raising the input parameter 100%.

Particle Phase

The radial variation of particle properties for the case 1 particle-laden jet is illustrated in Figs. 8 and 9 for $x/d = 20$ and 40. Predictions of the LHF and SSF models are shown on both plots. DSF predictions of $\tilde{G}$ and $\tilde{u}_p$ (the only particle parameters that this model provides) are also illustrated in Fig. 9. SSF predictions are in good agreement with data for all properties. An exception is the axial component of fluctuating

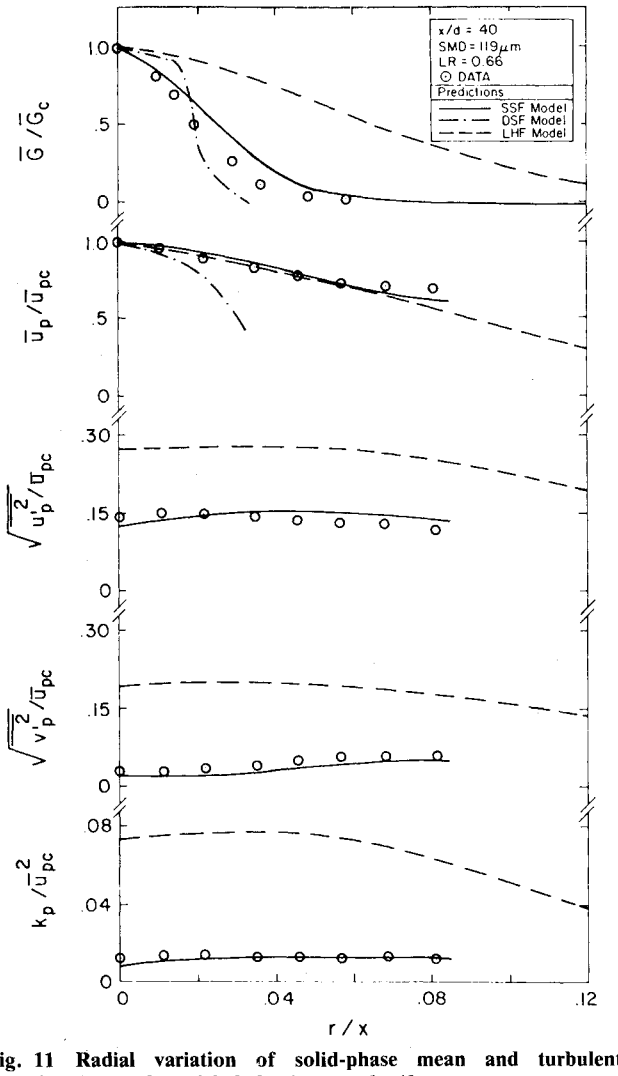

Fig. 11 Radial variation of solid-phase mean and turbulent quantities in case 3 particle-laden jet at $x/d = 40$.

velocity which is low near the axis and high near the edge of the flow. Predictions of the LHF model are not at all satisfactory, since neglect of particle inertia overestimates particle fluctuation levels and rates of spread. The DSF model yields poor results as well, since neglecting particle dispersion by turbulence causes the rate of spread of the particles to be substantially underestimated.

Similar results, at $x/d = 40$, for the case 2 and 3 particle-laden jets are illustrated in Figs. 10 and 11. The results are similar to Figs. 8 and 9 for the case 1 flow. The SSF model provides reasonably good predictions of all particle properties. The LHF model overestimates particle fluctuation and spread rates. The DSF model can predict only a few particle properties and these predictions are not very satisfactory since both particle spread rates and velocities are underestimated. A slight effect of loading ratio can be observed by comparing Figs. 10 and 11, where measured particle fluctuation levels are slightly lower near the axis for the jet having the higher loading ratio. The SSF model mimics this effect, even though effects of turbulence modulation are ignored for these computations. This occurs since the entire flow decays more slowly at higher loading ratios so that the particles tend to maintain lower fluctuation levels (representative of near-injector conditions) at each axial station.

Turbulence Modulation

Present data were not sufficient to determine $C_{\epsilon 3}$ accurately, which is needed to quantitatively allow for effects of turbulence modulation. Due to lack of other information, computations were undertaken by varying $C_{\epsilon 3}$ in the range 0.1-5. Results showed that changes in main flow properties, $\tilde{u}_c$, k_c, $(\overline{u'v'})_{\max}$, and G_c, were relatively small for present test conditions, e.g., always less than 10%.[8] Thus, in agreement with experimental observations, present test conditions were too dilute to provide a reasonable evaluation of $C_{\epsilon 3}$ or the turbulence modulation terms listed in Table 2. However, analysis of turbulence modulation helped to substantiate the dilute flow assumption of the present test flows.

Sensitivity Study

Specification of initial conditions is of vital importance to predictions using separated flow models; therefore, care was exercised to obtain reliable initial conditions for present test flows. However, uncertainties still exist in the specification of particle properties and initial conditions, e.g., particle size, since distributions were not exactly monodisperse; particle drag, since the particles were irregular; and ϵ_0, since it was not measured directly. Therefore, calculations were carried out to examine effects of varying these parameters on predictions.

Table 3 is a summary of a portion of the sensitivity results. The percent change in a given output parameter at $x/d = 40$ for a 100% increase in the input parameter is tabulated for the case 1 and 3 particle-laden jets (which are representative of all cases considered): The relative lack of sensitivity of gas-phase properties to parameter changes is clearly indicated. This is not surprising: as noted earlier, even changing the model had little influence on predictions of gas-phase properties.

The results appearing in Table 3 indicate that particle properties are more sensitive to parameter changes. The most influential parameter is particle size, next in importance is the drag coefficient. Even so, the standard deviations of the particle-size distributions in the present study are relatively small (in the range 11-23%); therefore, potential errors introduced by assuming monodisperse particle sizes are within experimental accuracy. Similarly, drag coefficients were calibrated and uncertainties in the drag should not result in predictions which have errors outside the limits of experimental accuracy.

Conclusions

The present measurements of the structure of particle-laden jets should be useful for evaluation of models of the process. The test conditions involve particle-laden flows where boundary-layer approximations apply with well-defined initial conditions, boundary conditions, and particle properties. Test conditions were chosen to provide significant effects of particle dispersion by turbulent fluctuations. The flows were dilute to facilitate measurements. All structure measurements, initial conditions, and particle-size distributions are tabulated in Ref. 8.

Major conclusions concerning the three models that were evaluated during this investigation are as follows:

1) The LHF and DSF models appear to have limited utility for modeling practical particle-laden flows. The LHF model overestimated flow development, since effects of slip are ignored, and performed well only for flows containing tracer-like particles during earlier work.[2] The DSF model generally underestimated the rate of flow development and particle dispersion, since effects of turbulent fluctuations are ignored, over the entire data base.

2) The SSF model, which allows for both particle slip and turbulent fluctuations, yielded reasonably good results over the entire data base (both existing[2,3] and present measurements) with no modification in the prescription for eddy properties from its original calibration.[2] This is encouraging, since the SSF method has the potential to treat nonlinear and complex interactions encountered in practical particle-laden flows, e.g., spray or particle drying and combustion.

3) Effects of turbulence modulation were small for the dilute particle-laden flows examined here; therefore, this aspect of the SSF model could not be evaluated adequately. The present approach is promising, however, since it only requires the determination of one new empirical constant for jet-like flows.

4) Sensitivity analysis indicated that the specification of particle properties exerts pronounced effects on predictions while initial gas-phase properties play a secondary role. This emphasizes the importance of measurements of initial particle-phase conditions and particle properties, e.g., drag and size, in order to obtain adequate evaluation of separated flow models.

Acknowledgment

This research was sponsored by the National Aeronautics and Space Administration, Grant NAG 3-190, under the technical management of R. Tacina of the NASA Lewis Research Center.

References

[1]Faeth, G. M., "Recent Advances in Modeling Particle Transport Properties and Dispersion in Turbulent Flow," *Proceedings of the ASME-JSME Thermal Engineering Conference*, Vol. 2, ASME, New York, March 1983, pp. 517-534.

[2]Shuen, J-S., Chen, L-D., and Faeth, G. M., "Predictions of the Structure of Turbulent, Particle-Laden, Round Jets," *AIAA Journal*, Vol. 21, Nov. 1983, pp. 1483-1484.

[3]Shuen, J-S., Chen, L-D., and Faeth, G. M., "Evaluation of a Stochastic Model of Particle Dispersion in a Turbulent Round Jet," *AIChE Journal*, Vol. 19, Jan. 1983, pp. 167-170.

[4]Al Tawell, A. M. and Landau, J., "Turbulence Modulation in Two-Phase Jets," *International Journal of Multiphase Flow*, Vol. 3, June 1977, pp. 341-351.

[5]Elghobashi, S. E. and Abou-Arab, T. W., "A Two-Equation Turbulence Model for Two-Phase Flows," *The Physics of Fluids*, Vol. 26, April 1983, pp. 931-938.

[6]Modarress, D., Wuerer, J., and Elghobashi, S., "An Experimental Study of a Turbulent Round Two-Phase Jet," AIAA Paper 82-0964, 1982.

[7]Modarress, D., Tan, H., and Elghobashi, S., "Two-Component LDA Measurement in a Two-Phase Turbulent Jet," AIAA Paper 83-0052, 1983.

[8]Shuen, J-S., Solomon, A. S. P., Zhang, Q-F., and Faeth, G. M., "A Theoretical and Experimental Study of Turbulent Particle-Laden Jets," NASA CR-168293, 1983.

[9]Solomon, A. S. P., Shuen, J-S., Zhang, Q-F., and Faeth, G. M., "Structure of Nonevaporating Sprays: Measurements and Predictions," AIAA Paper 84-0125, 1984.

[10]Szekely, G. A. Jr. and Faeth, G. M., "Reaction of Carbon Black Slurry Agglomerates in Combustion Gases," *Nineteenth Symposium (International) on Combustion*, The Combustion Institute, Pittsburgh, Pa., 1983, pp. 1077-1085.

[11]Shearer, A. J., Tamura, H., and Faeth, G. M., "Evaluation of a Locally Homogeneous Flow Model of Spray Evaporation," *Journal of Energy*, Vol. 3, Sept.-Oct. 1979, pp. 271-278.

[12]Mao, C-P., Szekely, G. A. Jr., and Faeth, G. M., "Evaluation of a Locally Homogeneous Flow Model of Spray Combustion," *Journal of Energy*, Vol. 4, March-April 1980, pp. 78-87.

[13]Lockwood, F. C. and Naguib, A. S., "The Prediction of the Fluctuations in the Properties of Free, Round Jet, Turbulent, Diffusion Flames," *Combustion and Flame*, Vol. 24, Feb. 1975, pp. 109-124.

[14]Gosman, A. D. and Ioannides, E., "Aspects of Computer Simulation of Liquid-Fueled Combustors," AIAA Paper 81-0323, 1981.

[15]Hinze, J. O., "Turbulent Fluid and Particle Interaction," *Progress in Heat and Mass Transfer*, edited by G. Hetsroni, S. Sideman, and J. P. Hartnett, Vol. 6, Pergamon Press, Oxford, 1972, pp. 433-452.

[16]Gosman, A. D., Lockwood, F. C., and Syed, S. A., "Prediction of a Horizontal Free Turbulent Diffusion Flame," *Sixteenth Symposium (International) on Combustion*, The Combustion Institute, Pittsburgh, Pa., 1977, pp. 1543-1555.

[17]Spalding, D. B., *GENMIX: A General Computer Program for Two-Dimensional Parabolic Phenomena*, Pergamon Press, Oxford, 1978.